PERGAMON

Atmospheric Environment 36 (2002) 2997–3008

ATMOSPHERIC ENVIRONMENT

www.elsevier.com/locate/atmosenv

Fumigation of pollutants in and above the entrainment zone into a growing convective boundary layer: a large-eddy simulation

X.-M. Cai[a,*], A.K. Luhar[b]

[a] *School of Geography and Environmental Sciences, University of Birmingham, Edgbaston, Birmingham B15 2TT, UK*
[b] *CSIRO Atmospheric Research, PMB 1, Aspendale, Vic. 3195, Australia*

Received 13 November 2001; received in revised form 28 February 2002; accepted 11 March 2002

Abstract

Fumigation of a passive plume located in or above the entrainment zone (EZ) into a growing convective boundary layer (CBL) has been simulated by large-eddy simulation (LES). Three non-dimensional parameters, $\alpha(=w_{e0}/w_{*0})$, z_0/z_{i0}, and σ_{z0}/z_{i0}, are used to classify different cases, where w_{*0} is the convective velocity scale, w_{e0} the initial entrainment velocity, z_{i0} the initial CBL height, z_0 the initial plume height, and σ_{z0} is the initial plume half-depth. Forty cases have been run and analysed. The crosswind-integrated concentrations have been compared with existing laboratory data from a saline convection tank. The results show that LES is a promising tool to reproduce fumigation processes. With a relatively coarse grid mesh near the EZ, LES derives reliable results that are in a good agreement with the laboratory data. The first parameter, α, containing the effects due to inversion strength, plays an important role in determining $C_0(T)$, the ground-level concentration (GLC) as a function of dimensionless time, T. For large α (say >0.03, corresponding to fast entrainment), variation of α gives significant change in $C_0(T)$; whereas for a wide range of α between 0.01 and 0.02 (corresponding to slow entrainment), $C_0(T)$ is almost independent of α. The starting time of fumigation does not vary significantly with the second parameter, z_0/z_{i0} (relative height of plume), although $C_0(T)$ is, in general, smaller for a higher plume. This confirms laboratory findings that the traditional notion of zero fumigation for a high plume (say above $1.10z_i$) is not correct. The effect of the third parameter, σ_{z0}/z_{i0}, is on the magnitude of $C_0(T)$; thinner initial plumes have higher GLCs.

Keywords: Coastal dispersion; Inversion break-up fumigation; Turbulent dispersion; Numerical simulation; Model comparison

1. Introduction

The fumigation phenomenon involves the entrainment of pollutants emitted in an overlying stably stratified layer into a growing convective boundary layer (CBL). The plume is brought downwards by convective eddies, which may cause high ground level concentrations (GLCs). In general, two types of fumigation are observed in the atmosphere: temporal inversion break-up fumigation and spatial advection fumigation. The former corresponds to a temporally growing CBL over a homogeneous surface that entrains a plume previously emitted into the inversion layer. The latter occurs if the inversion base varies spatially from place to place due to surface inhomogeneity (generally associated with a thermal internal boundary layer (TIBL), for example, near a shoreline or an urban area). When a plume of pollutant is emitted within a stable layer in one location with a lower inversion base and travels to another location with a higher inversion base above the plume height, fumigation takes place. Although these two types of fumigation possess different dimensions, similarity of the mechanisms that govern

*Corresponding author. Fax: +44-121-4145528.
E-mail address: x.cai@bham.ac.uk (X.-M. Cai).

1352-2310/02/$ - see front matter
PII: S1352-2310(02)00240-6

them allows translation from one to the other using Taylor's hypothesis. When such a translation is made, the start time of temporal inversion break-up fumigation is equivalent to the downwind distance for the start of spatial advection fumigation.

Some field studies have been carried out to investigate the mechanisms and the effects of fumigation. For example, two field studies of TIBL fumigation were reported by Lyons and Cole (1973) near Lake Michigan and by Misra and Onlock (1982) on the northern shore of Lake Erie. Their findings were limited by the impossibility of controlling experimental conditions within and above the TIBL. In contrast, the laboratory water-tank experiments by Deardorff and Willis (1982, hereafter DW82) have proved to be very successful. Two CBL growth rate conditions were examined in their study and the results revealed that the fumigation processes are significantly affected by the large amplitude of turbulent fluctuations in the entrainment zone (EZ) near the top of the CBL. More recent laboratory experiments have used a saline convective tank that was designed and constructed at CSIRO Atmospheric Research (Australia) in order to overcome some inadequacies of earlier designs and to provide access to a wider range of experimental conditions. Hibberd and Luhar (1996, hereafter HL96) used the tank to study the temporal break-up fumigation for a wide range of CBL growth rates.

Many applied models have been developed for describing fumigation. Most of these models are based on the assumptions of Gaussian dispersion profiles, smooth growth of the CBL or TIBL, and an instantaneous perfect vertical mixing of the entrained pollutants. However, problems with the assumptions in these simple models inevitably cause inaccuracy in the predicted pollutant GLCs (DW82). Another type of modelling technique, the Lagrangian particle model, has also been widely used in recent years, particularly as more computing resources have become available. Luhar and Britter (1990) used this type of model to examine fumigation in a coastal TIBL by considering turbulence inhomogeneity and skewness in the Langevin equation. For a simulation of plume fumigation associated with the morning break-up of the nocturnal inversion, Hurley and Physick (1991) showed that a relatively simple random walk model with homogeneous turbulence is able to reproduce results from the laboratory experiments of DW82.

Large-eddy simulation (LES) has advanced to a relatively mature level and is now widely accepted as a powerful numerical tool for describing the coherent structure of atmospheric turbulence. In general, applications of LES to the convective and the neutrally stratified boundary layers have been very successful (e.g., Mason, 1989; Cai and Steyn, 1996; Cai, 1999). Difficulties are encountered for stably stratified flows or flows near the ground because the turbulence possesses relatively small scales, and is intermittent and anisotropic in character. The subgrid-scale (SGS) schemes suitable for isotropic turbulence may not be appropriate for these flows. The dynamic SGS scheme (Germano et al., 1991) and backscatter approach (Mason and Thomson, 1992) have been proposed to improve the LES performance. There have been some attempts of LES to tackle stably stratified turbulence (e.g., Brown et al., 1994) using a backscatter SGS model. Recently, efforts have been made by Porte-Agel et al. (2000) to extend the dynamic SGS model so that the model coefficient is scale dependent. The model improved predictions of velocity spectra near the ground and has been evaluated by a sequence of field experiments, e.g. Porte-Agel et al. (2001).

There have not been many LES studies of entrainment until very recently. Sorbjan (1996a, b) carried out LES experiments to compare a penetrative CBL with a non-penetrative one by using a relatively small number of grid points ($32 \times 32 \times 55$ and $32 \times 32 \times 30$) and a coarse spatial resolution ($100\,\mathrm{m} \times 100\,\mathrm{m} \times 20\,\mathrm{m}$). Sullivan et al. (1998) used a nested LES to investigate the entrainment and flow structure in the inversion layer of a CBL over a range of bulk Richardson number (Ri) values. They found that the finite thickness of the inversion layer needs to be considered in an entrainment rate parameterisation to replace those derived using a jump condition.

Interestingly, an LES study of fumigation has not been carried out to date. One reason has been the uncertainty of a suitable grid resolution in the EZ. Very recently, Sullivan et al. (1998) and Stevens and Bretherton (1999) have addressed the grid-resolution issue and their conclusions may provide guidance to future LES of fumigation. The present study, as the first on LES of fumigation, aims to apply LES to temporal inversion break-up fumigation and, by comparing the results with the laboratory data of HL96, to explore the capability of LES.

2. Model configuration

The Colorado State University's Regional Atmospheric Modeling System (RAMS) was used to carry out the LES runs. The model contains a full set of non-hydrostatic compressible dynamic equations for major meteorological variables. An application of RAMS to LES of atmospheric turbulence was carried out by Cai and Steyn (1996) and Cai (1999, 2000). The LES configuration in the present study is similar to that in Cai (1999, 2000) except that a homogeneous surface is considered in this study. Smagorinsky's SGS model is employed and the model parameter C_s is taken as 0.1 for all cases. The model adopts a mesh of $64 \times 64 \times 52$ in

x-, y-, and z-directions, with the grid spacing being $60\,\mathrm{m} \times 60\,\mathrm{m} \times (2\text{–}30)\,\mathrm{m}$. Close to the ground, the vertical spacing is about 2 m, stretching, with a ratio of 1.15, upwards to a maximum spacing of 30 m. In this study, a "spin-up" run is conducted from $t = 0$ to 60 min. At $t = 0$ min, the potential temperature is specified as 293 K from the surface up to $z = 500$ m (the initial CBL height), with a stable stratification above with a lapse rate (i.e. vertical gradient) of potential temperature (LRPT) of $0.009\,\mathrm{K\,m^{-1}}$. No subsidence is specified during the whole simulation period. At the surface, a constant sensible heat flux of $0.0875\,\mathrm{K\,m\,s^{-1}}$ is specified. At $t = 60$ min, the CBL height (denoted by z_{i0}) simulated by LES reaches 640 m; hereafter we call this time the initial time, t_0. The CBL height is determined by finding the height at which the horizontally averaged sensible heat flux is a minimum near the EZ. At time t_0, an instantaneous *area* plume is inserted in the stable layer near the top of the CBL with a Gaussian concentration distribution in the vertical. Four different initial heights of the central plane of the area source, denoted by z_0, were used: 580, 640, 700, and 760 m. For each of these initial plume heights, two different plume half-widths were used: $\sigma_{z0} = 12$ and 30 m. Due to the finite vertical spacing at these heights, the Gaussian distribution with a half-width σ_{z0} of 12 m effectively becomes a top-hat distribution at one vertical grid (half-width of $0.5\Delta z$). At time t_0, the LRPT value above the CBL was re-assigned a new value from a selected set consisting of 0.002, 0.004, 0.005, 0.006, and $0.009\,\mathrm{K\,m^{-1}}$. The reason for re-assigning the LRPT value in the inversion layer is to test the effects of inversion strength on fumigation. This procedure slightly disturbs the dynamical balance at this moment, but the model quickly adjusts itself to the new balance.

For the present problem, the CBL has two velocity scales, the convective velocity w_* and the entrainment velocity w_e; and one length scale, the CBL height z_i. The variation in w_e depends on the LRPT value in the inversion layer, although its value is also influenced by w_*. The turnover time scale of a convective eddy with a typical size comparable to the CBL height is $t_* = z_i/w_*$. The CBL height z_i increases slowly with time (due to entrainment) on a time scale much larger than t_*, as does w_* (which is weakly dependent on z_i). We choose the values of w_*, z_i, and w_e at $t = 60$ min, namely, w_{*0}, z_{i0}, and w_{e0} as scaling parameters. The turnover time scale of convective eddies is then given by $t_{*0} = z_{i0}/w_{*0}$, which is used to scale the evolution of fumigation. The important dimensional parameters of the problem are: convective velocity scale, w_{*0}; initial entrainment velocity, w_{e0}; initial CBL height, z_{i0}; initial plume height, z_0; and initial plume half-width in the vertical, σ_{z0}. Based on dimensional analysis, these five dimensional parameters can be reduced to three non-dimensional parameters. A good choice for the three parameters is:

- non-dimensional entrainment rate $\alpha(= w_{e0}/w_{*0})$,
- non-dimensional initial plume height z_0/z_{i0},
- non-dimensional initial plume half width σ_{z0}/z_{i0}.

Specifying these three parameters defines the fumigation problem.

Table 1 gives the dimensional and non-dimensional parameters for all 40 cases studied. The first parameter, α, is the ratio of entrainment velocity to convective velocity and its value is determined by Eq. (3) in HL96. It can be shown that

$$\alpha = \frac{w_e}{w_*} \propto \left(\frac{w_*}{N z_i}\right)^2 = Fr^2,$$

where $N = ((g/\theta)(\partial\theta/\partial z))^{1/2}$ is the Brunt–Vasälä frequency and Fr is called the convective Froude number. When the LRPT in the inversion layer becomes large, one has the case of a non-penetrative CBL, for which $Fr \to 0$ and $\alpha \to 0$. Theoretically, when this happens, no fumigation would occur. When LRPT in the inversion approaches zero, one has the case of a CBL without a capping inversion, for which $Fr \to \infty$ and $\alpha \to \infty$. When this happens, the CBL grows extremely quickly and fumigation would occur rapidly. The second parameter, z_0/z_{i0}, represents the relative height of the initial plume. For pre-existing plumes in the inversion layer before any fumigation occurs, the CBL height is the only vertical length scale, as mentioned above; different initial elevations of the plume correspond to different starting times of fumigation and concentration fields should be identical except for a shift in time (with z_0 being the length scale for normalisation). In reality, however, plumes can be emitted into the EZ. In order to examine the fumigation processes for different initial heights, we

Table 1
Main parameters used for LES runs: w_{e0} is the entrainment velocity, w_{*0} is the convective velocity of the CBL, z_0 and σ_{z0} are the initial height and the vertical spread of the fumigating source, and z_{i0} is the initial CBL height

LRPT ($\mathrm{K\,m^{-1}}$)	0.002	0.004	0.005	0.006	0.009		
$\alpha = w_{e0}/w_{*0}$	0.055	0.027	0.022	0.018	0.012		
z_0 (m)	580	640	700	760	σ_{z0} (m)	12	30
z_0/z_{i0}	0.91	1.00	1.09	1.19	σ_{z0}/z_{i0}	0.036	0.092

specify four values for z_0/z_{i0}: 1.19, 1.09, 1.00, and 0.91. The first case with $z_0/z_{i0} = 1.19$ represents fumigation from above the EZ and the other three represent fumigation from within the EZ. For the same CBL, the case with a larger z_0/z_{i0} corresponds to a later and weaker fumigation. The third parameter, σ_{z0}/z_{i0}, represents the vertical spread of the plume. It should be noted that the vertically integrated amount of pollutant (denoted by Q_0 in units of mass per unit area) is the same for all cases with different σ_{z0}. All possible combinations of the three parameters in Table 1 have been run to give a total of 40 separate cases.

After the instantaneous area plumes are inserted at the given level, the LES is run for another 180 min. These results are analysed and discussed in the next section. Validation of the LES is made through a comparison with the experimental data reported by HL96.

3. Results and discussions

Our configured LES has no mean wind, and its dynamical setting is similar to the CBLs simulated in the thermal water-tank experiments of DW82 and the saline water-tank experiments of HL96. As far as the initial plume setting is concerned, the present model (area source) is different from those experiments, which used line sources. Cai (2000) used line sources to examine dispersion of passive plumes within the CBL, and the alignment of these instantaneous line sources corresponded to wind direction along which the results were integrated. The integration of concentration field yielded the concentration variation in the vertical and crosswind directions as a function of time. The present study, however, focuses on crosswind-integrated concentrations for a fumigation episode and does not examine crosswind dispersion. Because of this, an area source instead of a line source is employed. Using an area source results in as good results (of crosswind-integrated concentrations in the CBL or on the ground) as those derived from an ensemble average of a large number of line sources (Cai, 2000). This effectively enhances statistical accuracy and computational efficiency. A disadvantage of using an area source is that it does not provide characteristics of crosswind dispersion, but these were not presented in HL96.

There are slight differences between the definitions of z_{i0} (the initial CBL height) and t_0 (the starting time of fumigation) used by HL96 and the present study. In HL96, the fumigant ribbon was laid down in the stable layer and its height just before fumigation commenced defined the height z_{i0}. The time t_0 was then determined as "the earliest time at which downward diffusion was observed to occur along a significant length (about $0.5z_{i0}$) of the initial fumigant ribbon". In the present study, t_0 is specified as the time at which a fumigant sheet (i.e. area source) is inserted in the model domain and at which the CBL turbulence is fully developed; z_{i0} is then defined as the height of the minimum horizontally averaged sensible heat flux near the EZ at t_0. The present study does not follow the definitions by HL96 because difficulties and uncertainties in defining t_0 were encountered in both DW82 and HL96. LES has the advantages of a reliable specification of the CBL height and convenient insertion of a plume at any time and anywhere in the domain. It was, therefore, decided to make use of these advantages and to define z_{i0} and t_0 in a slightly different way in this study from that used in HL96. This causes slight differences when the LES results are compared with the laboratory results of HL96, as discussed below.

Fig. 1 shows an instantaneous view of dispersion 60 min after the source is inserted for the case with $\sigma_{z0}/z_{i0} = 0.036$, $\alpha = 0.012$, and $z_0/z_{i0} = 1.09$. Only two slices are shown, one horizontal plane at $z = 540$ m and the other vertical plane in the middle of the domain. Although it is 1 h after the insertion, the plume is still not fully fumigated due to its high elevation and the strong stability of the inversion. The vertical slice shows that near the places such as about one-fifth of the domain from the left, the plume has been entirely entrained. This shows that the strong updrafts are confined within some narrow zones and bring cleaner air from below; fumigation occurs near this zone while a nearby area may not be entrained significantly. Meanwhile, smaller scale turbulence together with SGS turbulence still contributes to downward dispersion for the section in which no large-scale updraft is observed. On the horizontal plane, we notice that near the updraft zones, concentrations are lower than surrounding areas

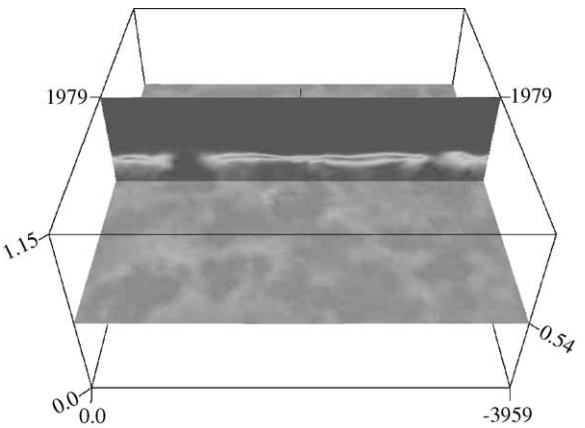

Fig. 1. A perspective view of concentration on two slices from the large-eddy simulation. The case is for parameters values of $z_0/z_{i0} = 1.09$, $\sigma_{z0}/z_{i0} = 0.036$ and $\alpha = 0.012$ and the time is 60 min after the source is inserted.

that are in general associated with slow-moving downdrafts. The length scale of such updrafts and downdrafts is purely determined by convective eddies in the CBL.

The results of fumigation derived from the present study are embedded in a time-varying frame. The results can, if necessary, be translated into a spatial-varying frame to correspond to shoreline fumigation. This requires the use of Taylor's hypothesis, which has been used in several previous studies including the measurement work of Willis and Deardorff (1978). Results averaged over a horizontal plane at time t for an *instantaneous area source* can be interpreted as crosswind-integrated concentrations at a downwind distance x for a *continuous point source*. Following the mixed-layer scaling proposed by Deardorff (1985), downwind distance x is scaled by $Ut_{*0} = Uz_{i0}/w_{*0}$, where U is the mean wind speed within the CBL, to form a dimensionless quantity $X = xw_{*0}/(Uz_{i0})$. When using Taylor's translation hypothesis to substitute x/U with the travel time of the plume, the dimensionless distance X is equivalent to the dimensionless time $T = t/t_{*0}$.

By integrating the concentration field over the whole horizontal plane at time t, we obtain a vertical profile of concentration $\bar{C}^{xy}(Z,T)$, where Z and T are normalised height and time. This is defined as

$$\bar{C}^{xy}(Z,T) = \frac{z_{i0}}{Q_0}\bar{C}^{xy} = \frac{z_{i0}}{Q_0}\frac{1}{L_xL_y}\int_0^{L_x}\int_0^{L_y} c(x,y,Z,T)\,\mathrm{d}x\,\mathrm{d}y, \qquad (1)$$

where $c(x,y,Z,T)$ is the dimensional concentration (mass per unit volume), L_x and L_y are the domain sizes along x- and y-directions, respectively, and Q_0 is the source intensity of the area plume (mass per unit area). With this definition, if the whole plume is fumigated into the CBL and well mixed, the value of $\bar{C}^{xy}(Z,T)$ will be unity, assuming the CBL height is still z_{i0}. When this quantity is applied to spatial advection fumigation, it is often referred to as the *crosswind-integrated concentration*. Another quantity discussed here is non-dimensional GLC, namely, $C_0(T) = \bar{C}^{xy}(0,T)$.

The left four panels (a)–(d) in Fig. 2 show the contours of $\bar{C}^{xy}(Z,T)$ derived from our LES for four different values of the entrainment parameter α, corresponding to four different inversion strengths, while the other two dimensionless parameters, z_0/z_{i0}, and σ_{z0}/z_{i0}, are fixed as 1.09 (initial plume core 9% above z_{i0}) and 0.036 (the thinner initial plume), respectively. For comparison, the right four panels (e)–(h) in Fig. 2 present the $\bar{C}^{xy}(Z,T)$ results given by HL96 for similar values of α to those in the left-hand panels. Panels (a) and (e) are cases with fairly "soft" inversions ($\alpha = 0.055$ for our LES and 0.068 for the HL96 laboratory study) with the CBL growing very fast. Consequently, fumigation occurs very rapidly, and the majority of the plume is entrained into the CBL. Because of this fast CBL growth, some portion of the plume is taken to higher levels, so that at later times (e.g., $T > 10$) the dimensionless concentration in the CBL only reaches about 0.6, not unity. As the CBL top grows quickly above the level of the initial plume core, the dispersion pattern for large values of T looks similar to the case with the plume source within the CBL (Nieuwstadt and de Valk, 1987), which have a typical downward motion of maximum concentration caused by skewed convective turbulence within the CBL. Therefore, for small T this case behaves like fumigation but for large T, it tends to have features of convective-driven dispersion. Comparing with the measured contours in Fig. 2(e), the present LES reproduces the main features of the dispersion well although the value of α is not exactly the same. In general, the value of $\bar{C}^{xy}(Z,T)$ from LES is higher than that from the experiments and this is partially attributed to a smaller value of α. It should be noted that the PDF model results given in HL96 also showed higher concentrations than the observations. It is also necessary to note the difference in the non-dimensional height of plume core between the left and right panels. As mentioned in the previous section, LES uses z_{i0} as the length scale to normalise the height while taking z_0/z_{i0} to be an independent parameter, but HL96 adopted the plume height z_0 as the length scale. This results in the plume core being at unity for the laboratory results and 1.09 for the LES results.

Panels (b) and (f) in Fig. 2 are for a slightly "harder" inversion (corresponding to a smaller entrainment rate) than those in panels (a) and (e); the value of α is 0.027 for LES and 0.022 for the laboratory experiments. Downward bending of the maximum $\bar{C}^{xy}(Z)$ occurs much later than in Figs. 2(a) and (e). Immediately below the core of the plume, the vertical gradient of $\bar{C}^{xy}(Z,T)$ is very large, but below $Z = 0.5$, the gradient is very small, indicating a well-mixed layer in the bottom-half of the CBL. It is interesting to observe a slight upward movement of the plume core with time. The water-tank experiment by HL96 also showed this feature (see Fig. 2(f) with $\alpha = 0.022$). This may be caused by negative skewness in the EZ (see Cai, 1999), which tends to disperse a symmetric distribution upwards, just the opposite of the dispersion effect in the middle of a CBL. Another possible explanation is that the LES produced a larger entrainment velocity than the experiments due to the coarse vertical grid resolution. Again, comparison between the LES results and the observations is reasonably good. A slight underestimation of GLCs for $10 < T < 15$ is partially attributed to a slightly larger value of α for the LES case.

For stronger inversions (see Fig. 2(c) for $\alpha = 0.018$ and Fig. 2(d) for $\alpha = 0.012$), the LES results still show the upward tilt of plume core. Downward bending of the maximum concentration zone also occurs later and the GLC does not reach its maximum before about $T = 15$.

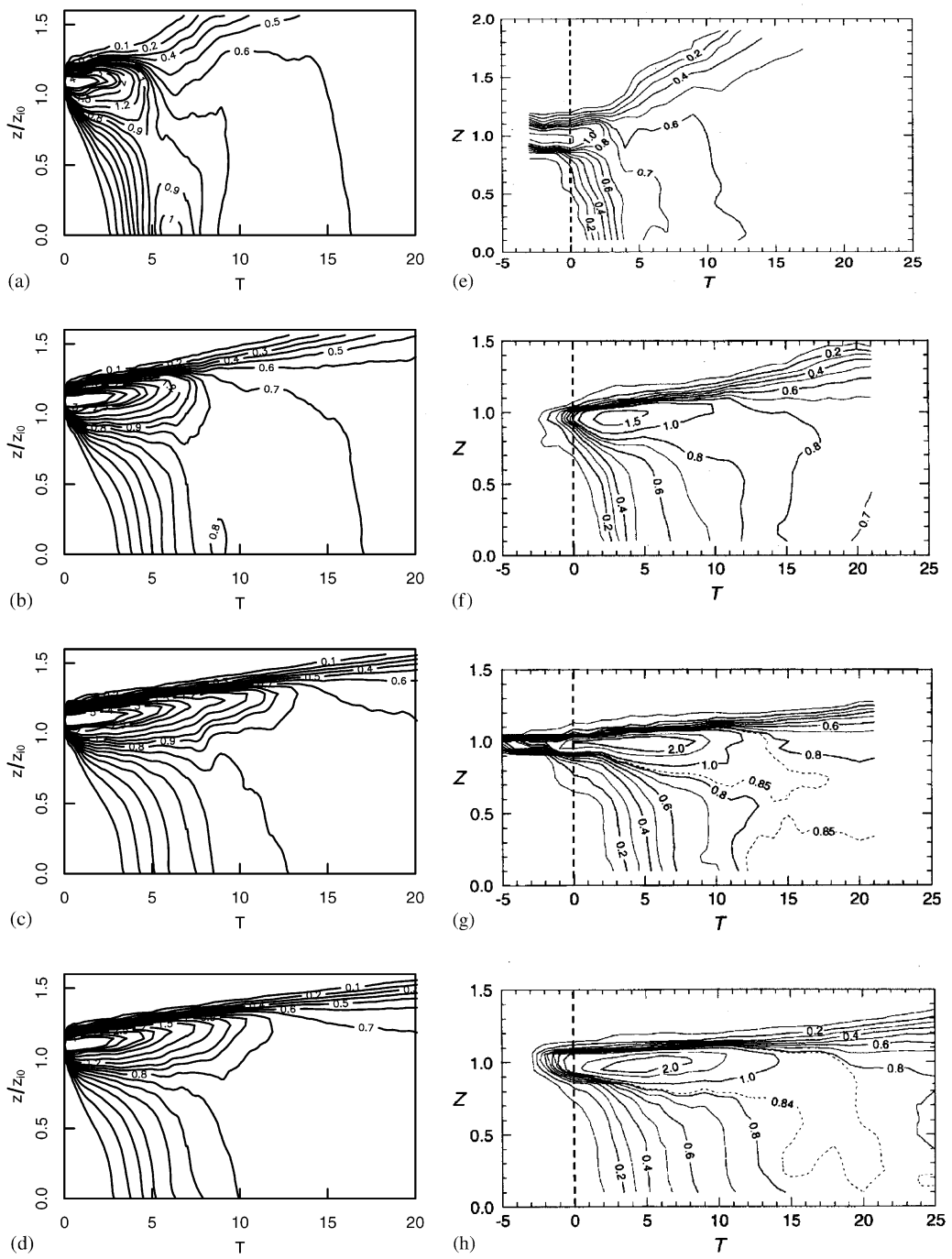

Fig. 2. Dimensionless crosswind-integrated concentration derived from LES (a)–(d) and from Hibberd and Luhar (1996) (e)–(h): (a) $\alpha = 0.055$; (b) $\alpha = 0.027$; (c) $\alpha = 0.018$; (d) $\alpha = 0.012$; (e) $\alpha = 0.068$; (f) $\alpha = 0.022$; (g) $\alpha = 0.014$; and (h) $\alpha = 0.010$. The LES cases (a)–(d) are for parameter values of $\sigma_{z0}/z_{i0} = 0.036$ and $z_0/z_{i0} = 1.09$. Each of the laboratory cases in (e)–(h) is an average of several experiments with slightly different values of σ_{z0}/z_{i0}. The vertical dashed line in (e)–(h) indicates the starting time of fumigation defined in HL96.

These match the results of HL96 shown in Figs. 2(g) and (h), which are for $\alpha = 0.014$ and 0.010, respectively. It should be noted that the results shown in Figs. 2(g) and (h) are averages of several experiments with slightly different parameters of σ_{z0}/z_{i0}. Therefore, a precise comparison between the LES and the laboratory data for $\bar{C}^{xy}(Z, T)$ is not possible. Despite this, the above-mentioned qualitative comparison has shown that LES of fumigation is very promising.

Fig. 3 compares GLCs predicted by the LES with the laboratory data. As far as the LES results are concerned, in order to show the transition from fumigation to dispersion of a plume emitted in the EZ near the top of the CBL, we include the two LES cases with $z_0/z_{i0} = 1.0$ and 0.91. The values of the parameter α for the laboratory data are not exactly the same as those in the LES, but the closest possible ones are chosen for each panel in Fig. 3. For example, the value of α for panel (a) is 0.055 for the LES and two sets of laboratory data are plotted with values of α equal to 0.068 (○) and 0.038 (△). These two observational data sets do not differ much except for small T during which more entrainment, therefore more fumigation, occurs to cause higher GLCs when α is larger. Both LES runs with initial plume heights 9–19% higher than z_{i0} are in good agreement with the tank data. For lower initial plume heights ($z_0/z_{i0} \leqslant 1.0$), the GLC increases rapidly at the beginning, typically with an overshoot maximum before dropping to an equilibrium level. This can be explained by the plume experiencing less small-scale mixing in the EZ before being brought to the ground in the large CBL downdrafts. For a higher initial plume ($z_0/z_{i0} > 1.0$), such overshooting is not very obvious and the maximum GLC occurs later than a case with a lower initial plume. After $T \approx 8$, the GLCs for all cases converge to one curve and this implies complete fumigation and mixing.

Although the well-mixed GLCs might be expected to equal unity, the asymptotic value of 0.5 shown in Fig. 3(a) is caused by the use of a constant CBL height, z_{i0}, as the length scale in Eq. (1). In this case with $\alpha = 0.055$, the inversion strength is weak and the CBL grows very quickly. At the end of the modelling period, the CBL height reaches about 1180 m, nearly double its initial height of 640 m (not shown here). It is, therefore, not surprising to have a value of normalised GLC of about 0.5 shown in Fig. 1(a). If the instantaneous value of the CBL height, $z_i(t)$, is used in Eq. (1), GLCs should approach unity at sufficiently large times. An example is shown in Fig. 4 for the cases in Fig. 3(a), but scaled by the instantaneous CBL height, $z_i(t)$. It should be noted

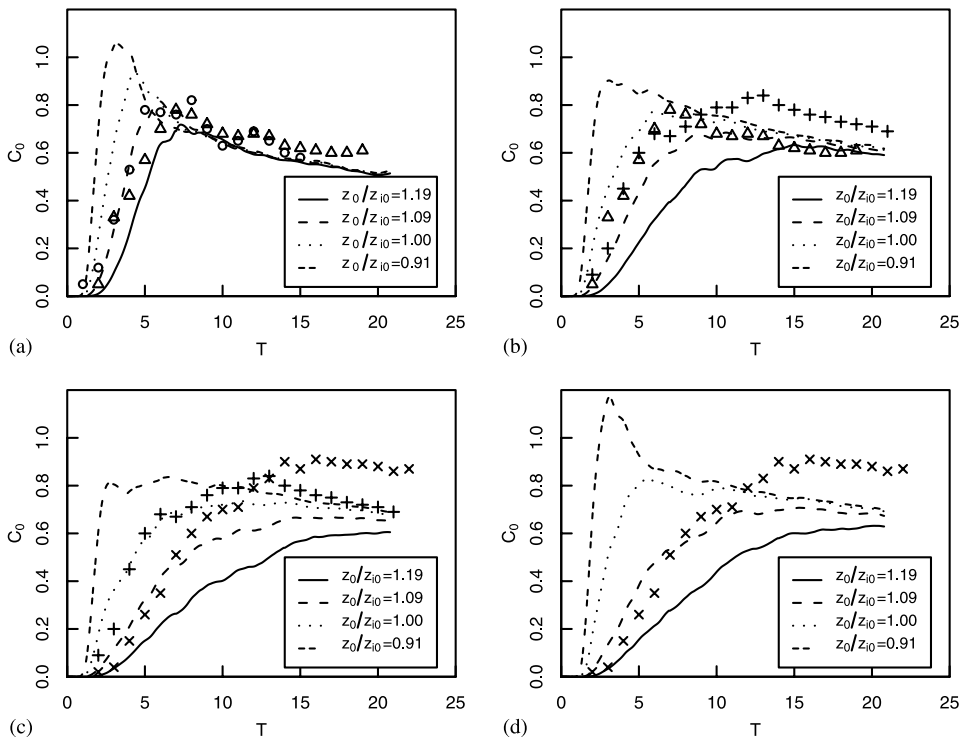

Fig. 3. Dimensionless GLCs as a function of dimensionless time for different initial heights of fumigant with $\sigma_{z0}/z_{i0} = 0.092$. (a) $\alpha = 0.055$; (b) $\alpha = 0.027$; (c) $\alpha = 0.018$; and (d) $\alpha = 0.012$. All the symbols are experimental data from HL96, namely: (○) $\alpha = 0.068$; (△) $\alpha = 0.038$; (+) $\alpha = 0.022$; (×): $\alpha = 0.014$.

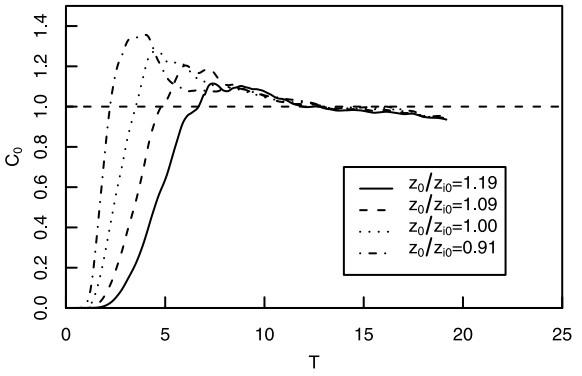

Fig. 4. Same LES results as those in Fig. 3(a), but scaled with instantaneous $z_i(t)$.

that T is still normalised by a constant $t_{*0} = z_{i0}/w_{*0}$, which is a function of z_{i0}. All cases now converge to unity, as the elapsed time is sufficiently large. Near the end of simulation, the GLC slightly drops below unity. This loss of fumigant attributed to the finite difference method (FDM) employed to discretise the diffusion processes, and possibly, to incomplete fumigation. The results indicate that these factors are not significant for the important initial details of the fumigation process. Although this analysis using the instantaneous $z_i(t)$ provides a validation of the simulation, it is more useful to scale using a constant z_{i0} because such results reflect the realistic GLCs (see the discussion in HL96). Therefore, GLCs shown hereafter in the present study are all scaled by a constant z_{i0}.

In Fig. 3(b), which shows the LES results for $\alpha = 0.027$, the experimental data for $\alpha = 0.038$ ($\triangle$) and 0.022 ($+$) are chosen for comparison. The two data sets are fairly close to each other for small T but approach different equilibrium values. Based on the above discussion, this is due to the slightly different CBL heights used to scale the GLCs. The case with a "softer" inversion ($\alpha = 0.038$, $\triangle$), or a larger entrainment rate, corresponds to a lower equilibrium GLC. It can be seen that the case with $z_0/z_{i0} = 1.09$ agrees well with the water-tank data for $\alpha = 0.038$ ($\triangle$). It seems that the observed GLCs rise earlier than the modelled ones before reaching their maxima. It is obvious that GLCs in the cases with high or low initial plume level ($z_0/z_{i0} = 1.19$ or $z_0/z_{i0} = 0.91$) deviate from the observed values quite significantly.

For $\alpha = 0.018$, the LES results are compared with the observations for $\alpha = 0.022$ ($+$) and 0.014 ($\times$) in Fig. 3(c). The two data sets are very different at both small and large times. At small times, the GLC starts to rise very slowly for the case with a "harder" inversion ($\alpha = 0.014$, $\times$), or a slower entrainment, and its equilibrium value is nearly 0.9. The model results for $z_0/z_{i0} = 1.09$ fit fairly well with the data for small times and all LES results converge to an equilibrium value of about 0.7, much lower than that attained by the experimental case with a "harder" inversion ($\alpha = 0.014$, $\times$). It seems that the LES results with $z_0/z_{i0} = 1.0$ match the observational data for $\alpha = 0.022$ ($+$). In general, LES results show that a peak in the GLC curve under fumigation conditions is not obvious for the case with a fairly "hard" inversion.

As the value of α is further decreased to 0.012, the emission height seems to become very important in terms of affecting GLCs, as shown in Fig. 3(d). A small change in the initial plume height causes significant differences in GLCs. The model results for $z_0/z_{i0} = 1.09$ fit the observational data for $\alpha = 0.014$ quite well for $T < 10$, but significantly underestimate them at later times. This deviation might partially be attributed to differences in the length scale used to normalise the results from LES and the tank experiments.

In Figs. 3(a)–(c), when the plume is released directly within the CBL ($z_0/z_{i0} = 0.91$) or within the EZ ($z_0/z_{i0} = 1.00$), the amount of overshoot in the GLC reduces as α decreases, but in Fig. 3(d) the overshoot is larger even though the value of α has reduced further. Given the type of scaling used, this feature can be explained in terms of three processes: (i) boundary-layer growth, (ii) entrainment (to cause initial emission to be diluted), and (iii) mixing within the boundary layer. For a source within the CBL, the maximum GLC has an overshoot above one (e.g. Cai, 2000). If the point source is within the EZ, a portion of the plume will be diluted somewhat before its mixing within the CBL, resulting in an effective reduction in the overshoot. When (i) dominates over (ii) and (iii)—the case in Fig. 3(a)—the growth of the CBL is rapid and the release from a source close to the CBL top effectively becomes that from a source lower within the boundary layer before the plume could diffuse significantly, and this causes an overshoot (e.g. Cai, 2000). When (i) is weaker—the cases in Figs. 3(b) and (c)—(ii) dominates over (i) and (iii) and it reduces the overshoot. When (i) is very weak—the case in Fig. 3(d)—(iii) dominates over (i) and (ii) and an overshoot appears again.

The above analysis only showed LES results with the thicker initial plumes ($\sigma_{z0}/z_{i0} = 0.092$). Notice that the value of σ_{z0}/z_{i0} in HL96 ranges from 0.017 to 0.043. In order to show the effects of the thickness of the initial plume on fumigation, a series of LES runs was carried out with thinner initial plumes, $\sigma_{z0}/z_{i0} = 0.036$. Comparison with the same laboratory data as used in Fig. 3 is shown in Fig. 5. In general, the modelled results are in slightly better agreement with the data, especially at large times. Panel (a) reveals a better agreement than in Fig. 3(a) for $T > 10$. This is attributed to a more complete fumigation that occurs with a thinner initial plume in the LES. In other words, slight

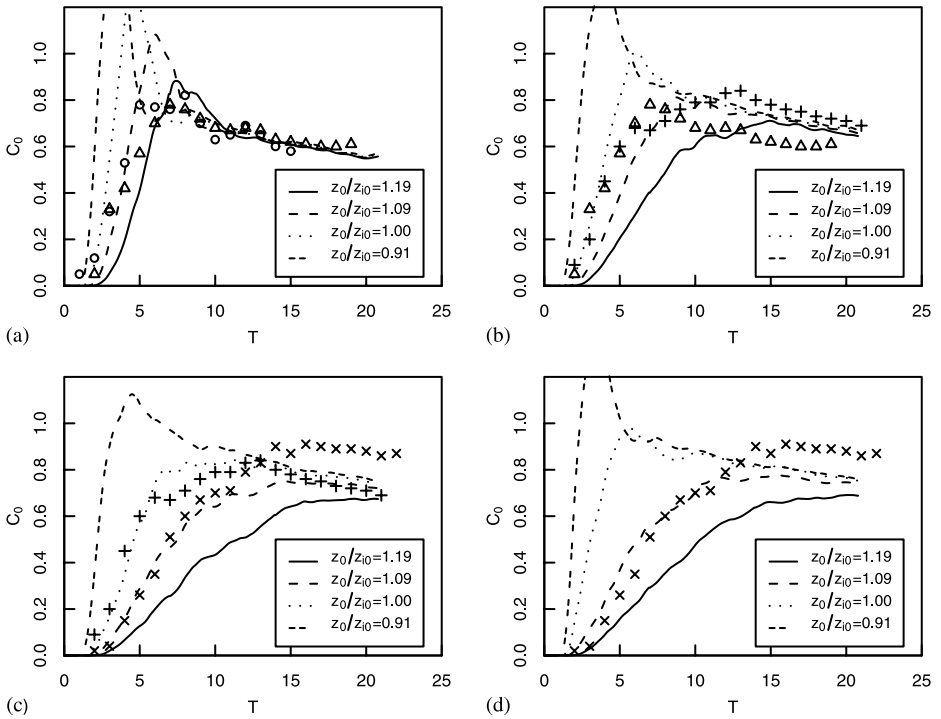

Fig. 5. Same as Fig. 3 but for $\sigma_{z0}/z_{i0} = 0.036$.

underestimation of equilibrium GLCs in Fig. 3 is partially because some, although a small, portion of the plume is still within the inversion layer and not fumigated into the CBL. Similar results are also found in Figs. 3(b)–(d).

The effects of the inversion strength on GLCs have been mentioned in the above discussions. However, the effects can be seen more clearly when the LES-produced GLCs for a set of α values are plotted together, as in Fig. 6. Firstly, when the inversion strength is weak, the GLC has a peak, as indicated by the solid curves in the figure. As the inversion strength increases, the overshoot in the GLCs disappears. Secondly, the difference in equilibrium GLC is inversely proportional to the difference in the instantaneous CBL height. Thirdly, there is no significant difference between the GLC curves when the value of α drops below a critical threshold of about 0.025. These findings may be helpful in constructing a parameterisation scheme for estimating GLCs under fumigation conditions.

The above results are based on the maximum vertical grid resolution of 30 m. In order to demonstrate the validity of this grid resolution for the application, the simulations with the maximum vertical grid resolution of 12 m (the total vertical grid number is 99) and $\alpha = 0.018$ have been conducted. Fig. 7 presents the comparisons between the two vertical grid resolutions for four cases. In general, the GLC is not very sensitive to the choice of the two grid resolutions. Using the higher resolution slightly reduces GLC values during the growing phase ($T < 10$) and this can be explained by a slightly lower CBL top associated with a smaller entrainment velocity due to the smaller grid spacing (Stevens and Bretherton, 1999). The difference between the GLC values for the two grid resolutions is more obvious for the thinner emission as shown in Fig. 7(c) and (d), but the difference is still relatively small.

4. Conclusions

Large-eddy simulation (LES) is used to simulate the fumigation of a passive source initially in or above the entrainment zone (EZ) of a growing convective boundary layer (CBL). The results are in a good agreement with experimental data obtained by Hibberd and Luhar (1996), while recognising that there are slight differences in the experimental settings, definition of starting time of fumigation, and the initial CBL height. The results suggest that a clearer definition of the starting time for a fumigation event is needed in order to make a meaningful comparison between the modelled output and experimental data. LES has the advantages of reliable quantification of the CBL height and convenient

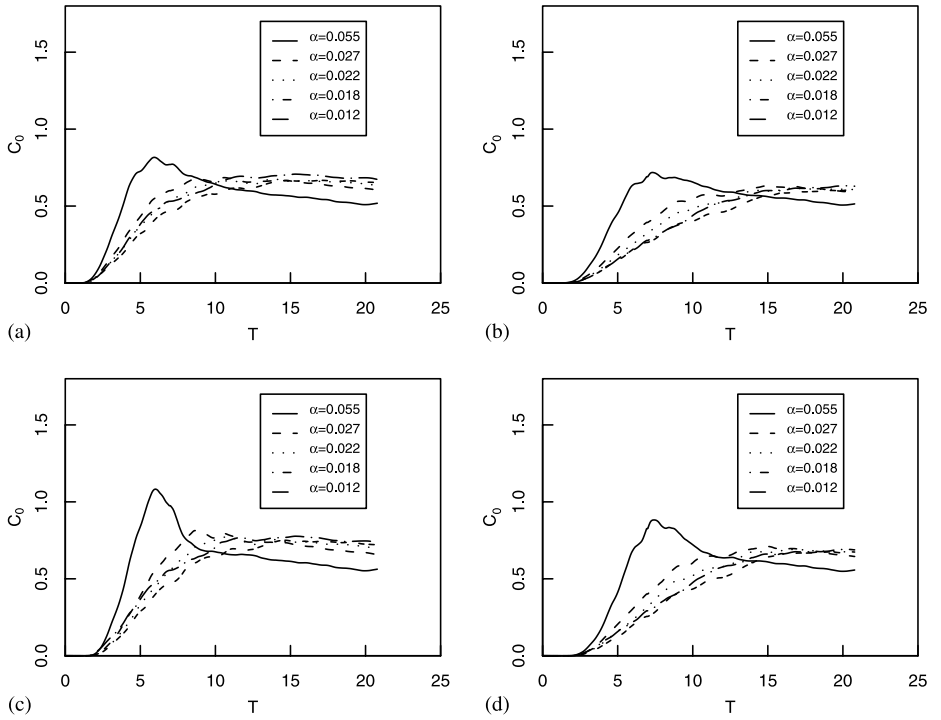

Fig. 6. Dimensionless GLCs as a function of dimensionless time for different values of α with: (a) $\sigma_{z0}/z_{i0} = 0.092$ and $z_0/z_{i0} = 1.09$; (b) $\sigma_{z0}/z_{i0} = 0.092$ and $z_0/z_{i0} = 1.19$; (c) $\sigma_{z0}/z_{i0} = 0.036$ and $z_0/z_{i0} = 1.09$; (d) $\sigma_{z0}/z_{i0} = 0.036$ and $z_0/z_{i0} = 1.19$.

insertion of a plume at any time and anywhere in the domain. The study makes use of these advantages to define z_{i0} and t_0 in a slightly different way from those used in HL96. These differences cause minor inconsistencies when the LES results are compared with the laboratory results in HL96.

The comparison between the LES results and the laboratory data shows that LES is capable of reproducing the main features of fumigation for a wide range of dimensionless parameters α, z_0/z_{i0} and σ_{z0}/z_{i0}. Among the three parameters, α is the most important one that controls entrainment processes and CBL growth. The results for the ground-level concentrations (GLCs) show that for a weak inversion above the CBL, variation of α causes a significant change in $C_0(T)$. However, when α is reduced to below 0.02, the effects are much weaker although the GLCs do not approach zero, as might be expected as α approaches zero if the EZ thickness also approaches zero. The second parameter, z_0/z_{i0}, appears to be nearly as important for the GLCs as α. Deardorff and Willis (1982) and HL96 showed that the simple notion of zero fumigation for a high plume (say above $1.10z_i$) is not correct; the LES results in the present study confirm this finding. Fumigation occurs for the case with $z_0/z_{i0} = 1.19$ almost immediately when the plume is inserted, regardless of the value of the other two parameters. This suggests that coherent eddies inside the CBL contain enough kinetic energy that the associated updrafts and downdrafts may entrain air parcels far above $1.10\ z_i$. The third parameter, σ_{z0}/z_{i0}, representing the initial size of the plume, also has some effect on fumigation, more specifically, on the magnitude of the GLCs; thinner (more concentrated) initial plumes lead to higher GLCs.

In this paper, the LES technique has been extended to describe the mean dispersion of fumigating plumes, which is a more complex dispersion problem than point-source dispersion in the CBL that has previously been addressed by various researchers using LES. The scaled results presented are applicable to both coastal fumigation and nocturnal inversion break-up fumigation. Given the success of the LES code used herein, it can be further used to investigate other topics on fumigation that would be very difficult to address through field or laboratory experiments due to the resources required. Such topics include the partitioning of total diffusion into meander and relative components for the concentration fluctuation problem, in-plume concentration fluctuation statistics, flow and turbulence properties within the rapidly evolving mixed layer and its growth,

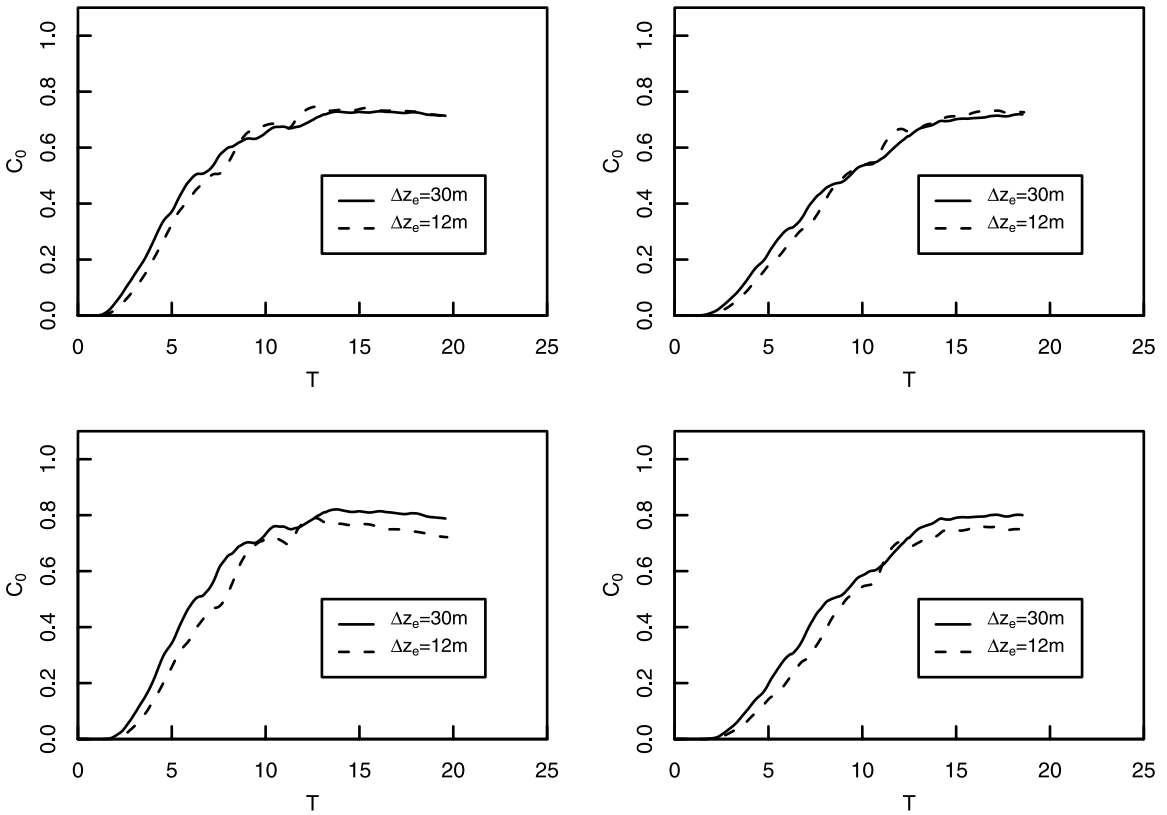

Fig. 7. Dimensionless GLCs as a function of dimensionless time for two vertical grid resolutions for $\alpha = 0.018$ with: (a) $\sigma_{z0}/z_{i0} = 0.092$ and $z_0/z_{i0} = 1.09$; (b) $\sigma_{z0}/z_{i0} = 0.092$ and $z_0/z_{i0} = 1.19$; (c) $\sigma_{z0}/z_{i0} = 0.036$ and $z_0/z_{i0} = 1.09$; (d) $\sigma_{z0}/z_{i0} = 0.036$ and $z_0/z_{i0} = 1.19$.

and properties and characteristics of the EZ in terms of its influence on the concentration distribution within the mixed layer.

Acknowledgements

The authors thank Dr. Mark Hibberd of CSIRO Atmospheric Research for providing a useful review of the manuscript. Many thanks to Roger Pielke of the Atmospheric Science Department at Colorado State University and Craig Tremback of ASTER, Mission Research Corporation, for providing the numerical code CSU-RAMS, version 2a. This research has been supported by the UK NERC funding.

References

Brown, A.R., Derbyshire, S.H., Mason, P.J., 1994. Large-eddy simulation of stable atmospheric boundary layers with a revised stochastic subgrid model. Quarterly Journal of the Royal Meteorological Society 120, 1485–1512.

Cai, X.-M., 1999. Large-eddy simulation of the urban convective boundary layer. Quarterly Journal of the Royal Meteorological Society 125, 1427–1444.

Cai, X.-M., 2000. Dispersion of a passive plume in an idealised urban convective boundary layer: a large-eddy simulation. Atmospheric Environment 34, 61–72.

Cai, X.-M., Steyn, D.G., 1996. The von Karman constant determined by large eddy simulation. Boundary-Layer Meteorology 78, 143–164.

Deardorff, J.W., 1985. Laboratory experiments on diffusion: the use of convective mixed-layer scaling. Journal of Climate and Applied Meteorology 24, 1143–1151.

Deardorff, J.W., Willis, G.E., 1982. Ground-level concentrations due to fumigation into an entraining mixed layer. Atmospheric Environment 16, 1159–1170.

Germano, M., Piomelli, U., Moin, P., Cabot, W.H., 1991. A dynamic subgrid-scale eddy viscosity model. Physics of Fluids A3, 1760–1765.

Hibberd, M.F., Luhar, A.K., 1996. A laboratory study and improved PDF model of fumigation into a growing convective boundary layer. Atmospheric Environment 30, 3633–3649.

Hurley, P., Physick, W., 1991. A Lagrangian particle model of fumigation by breakdown of the nocturnal inversion. Atmospheric Environment 25A, 1313–1325.

Luhar, A.K., Britter, R.E., 1990. An application of Lagrangian stochastic modelling to dispersion during shoreline fumigation. Atmospheric Environment 24A, 871–881.

Lyons, W.A., Cole, H.S., 1973. Fumigation and plume trapping on the shores of Lake Michigan during stable onshore flow. Journal of Applied Meteorology 12, 494–510.

Mason, P.J., 1989. Large-eddy simulation of the convective atmospheric boundary layer. Journal of the Atmospheric Sciences 46, 1492–1516.

Mason, P.J., Thomson, D.J., 1992. Stochastic backscatter in large-eddy simulations of boundary layers. Journal of Fluid Mechanics 242, 51–78.

Misra, P.K., Onlock, S., 1982. Modelling continuous fumigation of Nanticoke generating station plume. Atmospheric Environment 16, 479–489.

Nieuwstadt, F.T.M., de Valk, J.P.J.M, 1987. A large eddy simulation of buoyant and non-buoyant plume dispersion in the atmospheric boundary layer. Atmospheric Environment 21, 2573–2587.

Porte-Agel, F., Meneveau, C., Parlange, M.B., 2000. A dynamic scale dependent model for large eddy simulation: application to the neutral atmospheric boundary layer. Journal of Fluid Mechanics 415, 261–284.

Porte-Agel, F., Parlange, M.B., Meneveau, C., Eichinger, W.E., 2001. A priori field study of subgrid-scale heat fluxes and dissipation in the atmospheric surface layer. Journal of the Atmospheric Sciences 58, 2673–2698.

Sorbjan, Z., 1996a. Effects caused by varying strength of capping inversion based on large eddy simulation model of the atmospheric mixed layer. Journal of the Atmospheric Sciences 53, 2015–2024.

Sorbjan, Z., 1996b. Numerical study of penetrative and "solid-lid" non-penetrative convective boundary layers. Journal of the Atmospheric Sciences 53, 101–112.

Stevens, D.E., Bretherton, C.S., 1999. Effects of resolution on the simulation of stratocumulus entrainment. Quarterly Journal of the Royal Meteorological Society 125, 425–439.

Sullivan, P.P., Moeng, C.H., Stevens, B., Lenschow, D.H., Mayor, S.D., 1998. Structure of the entrainment zone capping the convective atmospheric boundary layer. Journal of the Atmospheric Sciences 55, 3042–3064.

Willis, G.E., Deardorff, J.W., 1978. A laboratory study of dispersion from an elevated source within a modelled convective planetary boundary layer. Atmospheric Environment 12, 1305–1311.